

Alma Mater Studiorum Università di Bologna
Archivio istituzionale della ricerca

Cooperativity and fragility in furan-based polyesters with different glycolic subunits as compared to their terephthalic counterparts

This is the final peer-reviewed author's accepted manuscript (postprint) of the following publication:

Published Version:

Fosse C., Esposito A., Thiyagarajan S., Soccio M., Lotti N., Dargent E., et al. (2022). Cooperativity and fragility in furan-based polyesters with different glycolic subunits as compared to their terephthalic counterparts. JOURNAL OF NON-CRYSTALLINE SOLIDS, 597, 1-11 [10.1016/j.jnoncrysol.2022.121907].

Availability:

This version is available at: <https://hdl.handle.net/11585/895886> since: 2022-10-12

Published:

DOI: <http://doi.org/10.1016/j.jnoncrysol.2022.121907>

Terms of use:

Some rights reserved. The terms and conditions for the reuse of this version of the manuscript are specified in the publishing policy. For all terms of use and more information see the publisher's website.

This item was downloaded from IRIS Università di Bologna (<https://cris.unibo.it/>).
When citing, please refer to the published version.

(Article begins on next page)

Cooperativity and fragility in furan-based polyesters with different glycolic subunits as compared to their terephthalic counterparts

Clément Fosse¹, Antonella Esposito^{1,*}, Shanmugam Thiyagarajan², Michelina Soccio^{3,4}, Nadia Lotti^{3,4,5}, Eric Dargent¹, Laurent Delbreilh^{1,*}

¹*Normandie Univ, UNIROUEN, INSA Rouen, CNRS, Groupe de Physique des Matériaux, 76000 Rouen, France*

²*Wageningen Food and Biobased Research, P.O. Box 17, 6700 AA Wageningen, The Netherlands*

³*Department of Civil, Chemical, Environmental and Materials Engineering, University of Bologna, 40131 Bologna, Italy*

⁴*Interdepartmental Center for Industrial Research on Advanced Applications in Mechanical Engineering and Materials Technology, CIRI-MAM, University of Bologna, 40126 Bologna, Italy*

⁵*Interdepartmental Center for Agro-Food Research, CIRI-AGRO, University of Bologna, 40126 Bologna, Italy*

Corresponding authors: antonella.esposito@univ-rouen.fr,
laurent.delbreilh@univ-rouen.fr

Abstract

This work aims to investigate the effect of the molecular groups found in polyester backbones (type of ring in the acidic subunit and length of the glycolic subunit) on the molecular dynamics. The investigation is done on three furan-based polyesters (PEF, PPF and PBF) as compared to their terephthalic counterparts (PET, PTT, and PBT) after full quenching from the molten state. The segmental molecular dynamics is investigated with MT-DSC, FSC and DRS. It is shown that the cooperativity decreases as the length of the glycolic subunit increases in both furan-based and terephthalic polyesters. No direct correlation between the fragility index and the cooperativity is observed in furan-based polyesters containing glycolic subunits of different lengths. The differences in the isochoric fragilities obtained for the furan-based polyesters and their terephthalic counterparts has been assumed to result from the combination of backbone flexibility and packing efficiency of the macromolecular chains

in the amorphous phase.

Keywords: molecular mobility, bio-based polyesters, dielectric relaxation spectroscopy, fast scanning calorimetry, backbone flexibility, packing efficiency

1. Introduction

New polymers are constantly being synthesized from sustainable resources to replace fossil-based materials. Currently, one of the most promising biosourced chemicals is furandicarboxylic acid (FDCA), which can be produced from vegetable feedstock and used to synthesize polyesters through the combination with different diols, allowing to obtain repeating units with glycolic subunits of different lengths. For example, poly(ethylene furandicarboxylate) (PEF) is obtained by combining FDCA with ethylene glycol, poly(propylene furandicarboxylate) (PPF) is obtained by combining FDCA with 1,3-propanediol, poly(butylene furandicarboxylate) (PBF) is obtained by combining FDCA with 1,4-butanediol [1], and so on. It is worth noting that FDCA exists in the form of three position isomers [2], but the most commonly used is 2,5-FDCA. Among all the mentioned furan-based polyesters, 2,5-PEF is the most studied due to some interesting mechanical and barrier properties, which makes it the best potential bio-based surrogate to poly(ethylene terephthalate) (PET) for packaging [3]. 2,5-PPF is also an interesting polymer with excellent gas barrier properties [4], which makes it a promising substitute for its petroleum-based homologues poly(trimethylene terephthalate) (PTT) and poly(trimethylene naphthalate) (PTN) in packaging applications. Another polymer belonging to the family of furan-based polyesters and worth investigating is 2,5-PBF. This polymer has good thermal, mechanical and barrier properties [5], and could therefore be suitable for food-packaging applications in replacement of its terephthalic counterpart. But before making decisions on whether a polymer can be substituted by another polymer, it is of uppermost importance to have an idea of the potential properties of these promising materials, both in the amorphous state and in the presence of semi-crystalline structures. The literature reports that the presence of a rigid

amorphous fraction has a strong effect on the mechanical and barrier properties of semi-crystalline polymers [6, 7, 8, 9, 10], but polymer microstructures can be quite complex [10], and before investigating semi-crystalline samples it may be worth evaluating the molecular mobility of the fully amorphous samples. Investigations of the molecular mobility in amorphous biobased 2,5-PEF and 2,4-PEF as compared to poly(lactic acid) (PLA) and PET, for instance, allowed making a correlation between the glass-forming behaviour of 2,5-PEF and its particularly high value of the dielectric strength with the dipolar moment, the packing efficiency of the macromolecular chains, and therefore the free volume and the barrier properties [11]. Similar investigations performed on a series of amorphous biobased copolyesters obtained with both 2,5- and 2,4-FDCA showed that position isomerism affects the glass transition temperature and the relaxation times associated with the β relaxation processes, but has no obvious effects neither on the fragility index, nor on the cooperativity [12]. Guidotti et al. [13] recently synthesized and characterized a series of four homopolyesters of 2,5-FDCA with glycols of different lengths (i.e. with a number of methylene groups in the glycolic subunit going from 3 to 6). They concluded that the length of the glycolic subunit is a key parameter in determining the kind and fraction of ordered phases developed by the samples during compression molding followed by cooling. They evidenced the formation of a less-ordered (one- or two-dimensional) phase (they called it "mesophase") that, together with the amorphous and the eventually present crystalline phase, significantly impacted the mechanical and barrier properties. Soccio et al. [14] investigated the molecular dynamics of these four poly(alkylene 2,5-furanoate)s and unveiled complex local relaxations (characterized by the simultaneous presence of two components depending on the thermal treatment), plus a segmental relaxation whose relaxation time and strength depended on the glycolic subunit length. In another work, Martínez-Tong et al. [15] reported on the molecular origin of some peculiar physical properties of poly(pentamethylene 2,5-furanoate), observing that the molecular dynamics in polymers can be sensitive to thermal history over a broad temperature range even in the noncrystallized state, due to a possible

modulation of the interchain interactions. This further stresses the relevance of investigating polymers in their fully amorphous state prior to evaluate the effect of crystallization. Genovese et al. [16] had previously investigated the effects of chemistry (nature and structure of the ring in the acidic subunits) on the relaxation dynamics of three polyesters, comparing the furan, the terephthalic and the cyclohexane rings, but only focused on the subglass secondary relaxation modes. The advantage of comparing polyesters with different rings is that the corresponding polymer backbones have different flexibilities and can be either aromatic or fully aliphatic. They evidenced a multimodal nature of the subglass T_{beta} process, detecting three modes for the more flexible polyester (with cyclohexane rings) but just a single mode for the stiffer polyester (with furan rings).

The molecular mobility of polymers in the temperature range corresponding to their glass transition can be described using the approach proposed by Adam and Gibbs [17]. In this approach, the segmental relaxation processes are occurring in so-called Cooperative Rearranging Regions (CRRs). A CRR is defined as the smallest subsystem in which the α -relaxation process can occur independently of the neighboring subsystems; each CRR is characterized by its own relaxation dynamics and thermodynamic variables. An experimental method has been proposed by Donth [18, 19] to estimate the average size of a CRR from calorimetric measurements using equation 1.

$$\xi_{T\alpha}^3 = \frac{1/(C_p)_{solid} - 1/(C_p)_{liquid}}{\rho(\delta T)^2} k_B (T_\alpha)^2 \quad (1)$$

Where C_p is the isobaric heat capacity, k_B is the Boltzmann constant, ρ is the polymer density, δT_g is the average temperature fluctuation within a CRR and T_α is the dynamic glass transition temperature. Donth's approach allows to estimate the average CRR size at the glass transition temperature exclusively from calorimetric experiments. Previous studies led to the development of a method to determine the average CRR size on a wider frequency range, providing access to a more complete spectrum of the structural relaxation. The method proposed by Saiter et al. [20] combines Dielectric Relaxation Spectroscopy (DRS)

and Modulated-Temperature Differential Scanning Calorimetry (MT-DSC) to estimate the CRR size over an extended temperature and frequency range, from the cross-over region through the glass transition.

90 Cooperativity has been proven to depend not only on temperature, but also on structural constraints such as confinement effects [21, 22, 23, 24]. Numerous studies have also shown that the cooperativity length ξ_α can be highly affected by changes in the intermolecular interactions, e.g. in the presence of a plasticizer or when the polymer backbone bears side chains having different lengths, 95 or simply due to different macromolecular arrangements [25, 26, 27, 28]. Nakaniishi et al. [29] proposed a simplified model of hydrogen-bond network based on polyhydric alcohols, and used the Adam and Gibbs' approach to show that the average CRR size increases when the intermolecular interactions increase. Some attempts have also been made to correlate a change in the CRR size with the 100 evolution of the relaxation times. Hong et al. [30] investigated a wide range of glass-forming liquids including polymers, but observed no evident correlation between the cooperativity length and the fragility index. They explained this discrepancy by splitting the fragility index into two contributions, one measured in isochoric conditions m_v and one only due to volume changes ($m - m_v$). Under 105 this assumption, the fragility m can be expressed using equation 2:

$$m = (m - m_v) + m_v = \frac{\Delta V^\#}{\ln(10)k_B} \frac{\alpha_T}{\kappa} + m_v \quad (2)$$

Where α_T is the thermal expansion coefficient of the supercooled liquid at the glass transition temperature, κ is the compressibility, and $\Delta V^\#$ is approximately equal to 4% of the cooperativity volume. For a wide range of glass-forming liquids including polymers, α_T/κ is comprised between 0.5 and 3 $MPaK^{-1}$ [30].

110 According to the literature, only the parameter ($m - m_v$) should be straightly correlated to the cooperativity at the glass transition [30, 28]. As a consequence, fragility and cooperativity are expected to be correlated only when the isochoric fragility m_v remains constant.

Recently, Araujo et al. [31] proposed a structural interpretation of the two 115 contributions governing the fragility in polymer systems. According to their

results, $(m - m_v)$ depends on the inter-chain interactions, whereas the isochoric fragility m_v mainly depends on the backbone stiffness. It is therefore likely that any change in the inter-chain interactions induced by structural changes that do not affect the backbone stiffness also lead to a concomitant evolution of fragility and cooperativity. A more recent study from Araujo et al. [25] on plasticized PLA showed that a change of inter-chain interactions induced by the incorporation of a plasticizer results indeed in a correlated evolution of cooperativity and dynamic fragility.

This work aims to investigate the effect of the molecular groups found in polyester backbones (type of ring in the acidic subunit and length of the glycolic subunit) on the molecular dynamics of three furan-based polyesters (2,5-PEF, 2,5-PPF, and 2,5-PBF, simply referred to as PEF, PPF and PBF in the following) as compared to their terephthalic counterparts (PET, PTT, and PBT) after full quenching from the molten state. The segmental molecular dynamics have been investigated through the concept of cooperativity as defined by Adam and Gibbs [17]. Cooperativity has been estimated using MT-DSC according to Donth's model [18, 19]. The approach proposed by Hong et al. [30] has been used to determine the two fragility contributions and then estimate any possible correlation between cooperativity and fragility. The discussion has been focused on the values of isochoric fragility m_v to get a better understanding of the parameters potentially affecting the properties of the investigated polymers.

2. Materials and Methods

2.1. Materials

Poly(ethylene 2,5-furandicarboxylate) (PEF), poly(butylene 2,5-furandicarboxylate) (PBF) and poly(trimethylene terephthalate) (PTT) were synthesized in the Food and Biobased Research (FBR) laboratories located in Wageningen, the Netherlands, according to procedures previously reported in the literature [32, 1, 33, 34]. Poly(propylene 2,5-furandicarboxylate) (PPF) was synthesized in

145 the Department of Civil, Chemical, Environmental and Materials Engineering
(DICAM), University of Bologna, Italy, according to the procedure reported
in [35]. Poly (ethylene terephthalate) (PET) and poly(butylene terephthalate)
(PBT) are industrial grades and were purchased. Prior to measurement, all the
samples were stored in a desiccator with P_2O_5 for at least 24h. The samples
150 are listed in Table 1.

2.2. Modulated-Temperature Differential Scanning Calorimetry (MT-DSC)

MT-DSC experiments were performed on a Q100 (TA Instruments) using
the Tzero Technology. Prior to measurement, energy, temperature and heat
capacity calibrations were carried out using indium and sapphire standards.
155 Every experiment was achieved under a constant nitrogen flow of 50 mL min^{-1}
to avoid oxidative degradation of the samples. The samples were first melted
within their MT-DSC pan using a hot plate at a temperature above their melt-
ing temperature, and then quenched on a cold plate to obtain fully amorphous
samples. After quenching, a heat-only protocol starting from -70°C to a tem-
160 perature above the melting temperature was applied to each sample. According
to [36], the measurements were performed with a heating rate of 2K min^{-1} , a
modulation amplitude of $\pm 0.318\text{K}$ and a period of 60s.

2.3. Fast Scanning Calorimetry

FSC experiments were carried out using a Flash-DSC1 calorimeter (Mettler-
165 Toledo) equipped with a HUBER TC100 intracooler. Prior to measurement,
each MultiSTAR UFS1 MEMS empty chip was conditioned and corrected ac-
cording to the manufacturer recommendations. During the analysis, a constant
nitrogen flow of 200 mL min^{-1} was used to prevent any oxidative degradation
of the samples. The dynamic thermal lag depends on the selected heating (and
170 cooling) rate [37]; in this work it was measured at $\beta^h = |\beta^c| = 1000\text{K s}^{-1}$. The
static thermal lag ΔT_S depends on the sample thickness and was calculated as
a third of the distance between the melting temperatures of two indium pieces,
one placed on the reference sensor and the other placed on top of the sample

[37]. To prevent thermal gradients and ensure small values of static thermal
 175 lag, all the samples were prepared with a thickness not exceeding $10 \pm 3 \mu m$ as
 recommended by Toda et al. [38], and placed in the middle of the sensor as
 advised by Jariyavidyanont et al. [39]. The sample masses ranged between 14
 ng (PEF) and 38 ng (PBF) and were measured by using equation 3:

$$m = \frac{(\Delta C_p)_{am}^{FSC}}{(\Delta C_p)_{am}^{MT-DSC}} \quad (3)$$

Where $(\Delta C_p)_{am}^{FSC}$ is the heat capacity step at the glass transition estimated
 180 by FSC ($\beta^h = 1000K s^{-1}$) and $(\Delta C_p)_{am}^{MT-DSC}$ is the heat capacity step at
 the glass transition measured by MT-DSC ($\beta^h = 2K min^{-1} \approx 0.033K s^{-1}$) on
 the sample in its reference amorphous state.

2.4. Dielectric Relaxation Spectroscopy (DRS)

DRS experiments were performed using interdigitated electrodes (BDS 1410-
 185 20-150) from Novocontrol Technologies GmbH (accuracy in $\tan \delta \approx 0.001$, sensor
 diameter 20 mm and combs-gold plated copper). The combs fingers are $150 \mu m$
 in width and $35 \mu m$ in thickness and are spaced by $150 \mu m$. Prior to sample
 deposition, the electrodes were calibrated by determining their respective geo-
 metric (empty) capacity (C_0) and substrate capacity (C_{SU}) through measure-
 190 ments of a reference material of known permittivity (hydroxy-terminated PPMS,
 Sigma Aldrich). After the sample deposition, the electrodes were heated on a
 hot plate to melt the polymer samples before quenching them on a cold plate.
 The measurements were then carried out in a frequency range of 10^{-1} – 10^6 Hz by
 an Alpha-A analyzer (Novocontrol Technologies GmbH). A Quatro Cryosystem
 195 (Novocontrol Technologies GmbH) was used to control the temperature with a
 stability of $\pm 0.5^\circ C$. The temperature was increased from $-150^\circ C$ to $150^\circ C$ using
 appropriate steps. The Havriliak-Negami (HN) complex function was used to
 analyze the dielectric relaxation curves:

$$\varepsilon^*(\omega) = \varepsilon_\infty + \frac{\Delta\varepsilon_{HN}}{[1 + (i\omega\tau_{HN})^{\alpha_{HN}}]^{\beta_{HN}}} \quad (4)$$

Equation 4 allows to fit the real and imaginary components (respectively $\varepsilon'(\omega)$ and $\varepsilon''(\omega)$) of the complex dielectric permittivity ($\varepsilon^*(\omega)$). From the fitting results it is possible to estimate the relaxation strength $\Delta\varepsilon_{HN}$, the relaxation time τ_{HN} , and the symmetric and asymmetric broadening factors α_{HN} and β_{HN} of the α and β relaxation processes [40, 41].

3. Results and Discussion

Figure 1 shows the Reversing Heat Capacity signals obtained from MT-DSC measurements at a heating rate of $2K\ min^{-1}$ on the fully amorphous samples, except for the PBT sample for which quenching was not successful. With this only exception, all the samples showed a clear glass transition step followed by a cold crystallization peak, and a melting peak corresponding to the crystalline phase formed during the heating ramp. The enthalpies of crystallization and melting were systematically compared to confirm that the samples were fully amorphous in their initial state, i.e. right after quenching, at the beginning of the heating ramp. Table 2 reports the thermal parameters extracted from

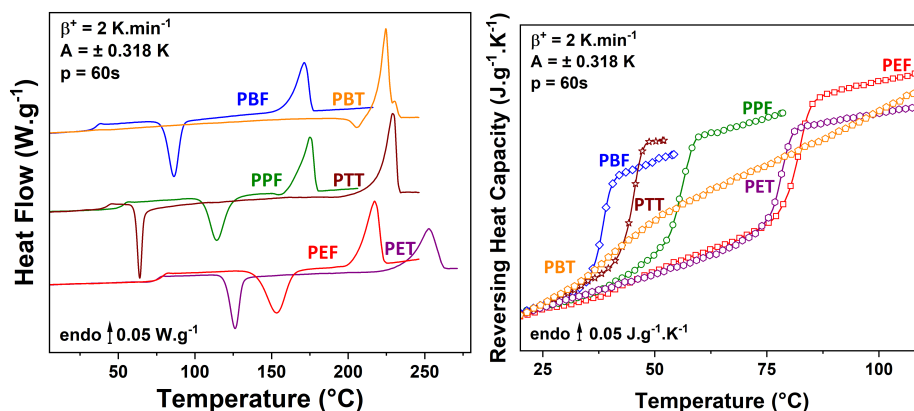


Figure 1: Heat Flow and Reversing Heat Capacity signals measured on the quenched (fully amorphous) samples using a heat-only MT-DSC protocol. Quenching was not successful for the PBT sample.

Figure 1. According to the literature [42, 43, 44, 45], at least two crystalline phases can be observed in furan-based polyesters. The α' crystals formed at low

temperatures are imperfect, and therefore prone to melt-recrystallization processes during heating; the α crystals formed at higher temperatures are more perfect [43]. For all samples, the cold crystallization temperature corresponds to the temperature at which the less perfect α' crystals are formed, whereas
220 the melting temperature is associated with the melting of the more perfect α crystals. This means that, when the initially amorphous samples are heated up, they crystallize into α' crystals and then reorganize into α crystals. At low scanning rates, the crystalline reorganization processes are possible and the measured enthalpies of melting are consequently affected by significant uncer-
225 tainties. Table 2 shows that for both furan-based and terephthalic polyesters, an increase in the length of the glycolic subunit produces a decrease in the glass transition temperature, as well as a decrease in both the cold crystallization and melting temperatures. The literature reports that a decrease is observed in the characteristic temperatures when the length of the glycolic subunit increases,
230 and that this phenomenon should be attributed to an increased flexibility of the polymer chains [46, 47]. The increased chain flexibility would also explain the width reduction of the cold crystallization peak. The width of a crystallization peak generally indicates how fast the crystallization process occurs; this work suggests that an increased length of the glycolic subunit produces an increase
235 in the crystallization rate. It is therefore quite straightforward to expect that a significant change in the molecular mobility in the amorphous phase should be observed depending on the length of the glycolic subunit.

For terephthalic polyesters and other polymeric systems containing n methylene units in their backbone, the literature reports that the melting temperature fol-
240 lows a so-called even-odd effect [48, 49, 13]. This effect is due to the fact that the melting temperature is not only related to the flexibility of the polymer chains, but also to the chain conformations and to the crystal structure [49]. The even-odd effect has recently been reported in furan-based polymers with a higher number of methylene units (up to 12) by Papamokos et al. [46]. They
245 showed that the polymers with an odd number of methylene units are not able to crystallize when heated at a rate of 10 K min^{-1} after melt quenching. This

finding indicates that the polymers containing an odd number of methylene units have a lower crystallizability, i.e. crystallization occurs at a lower rate as compared to those containing an even number of methylene units. In a following work Guidotti et al. [13] reported that, after storage at room temperature for one month, only the 2,5-FDCA-based homopolymers containing an even number of $-\text{CH}_2-$ groups in the glycolic subunit (poly(butylene 2,5-furanoate) with $n = 4$ and poly(hexamethylene 2,5-furanoate) with $n = 6$) were able to develop a three-dimensional ordered crystalline phase, the other two (poly(propylene 2,5-furanoate) with $n = 3$ and poly(pentamethylene 2,5-furanoate) with $n = 5$) remained completely amorphous. Table 2 shows that, for both furan-based and terephthalic polyesters, an increased length of the glycolic subunit leads to a decrease in the glass transition temperature (measured as the midpoint of the glass transition) that can be attributed to the increased flexibility of the polymer chains. It also appears that the furan-based samples tend to have higher glass transition temperatures with respect to their terephthalic counterparts, except when the number of methylene groups is equal to 4. These findings suggest that the furan-based samples have a less flexible backbone and/or develop stronger intermolecular interactions with respect to their terephthalic counterparts. In a recent study comparing the chain motions in PEF and PET, Burgess et al. [3] showed that the furan ring-flipping motions are largely suppressed due to the non-linear axis of ring rotation in addition to a strong ring polarity, which is not the case of the phenyl ring-flipping motions in PET. This further supports the fact that PEF has a less flexible backbone with respect to PET.

The cooperativity length at the dynamic glass transition (ξ_α) has been estimated for all the samples by using equation 1. From the literature, the possible changes in the CRR size are generally attributed either to chemical and/or physical modifications of the intermolecular interactions [50, 30, 26, 27, 25, 28], or to confinement effects [23, 22, 21]. Table 2 shows that the CRR size decreases as the length of the glycolic subunit increases in both furan-based and terephthalic polyesters. The average CRR size for PBT is much lower compared to PET and PPT because the PBT sample investigated in this work is indeed

semi-crystalline (quenching from the melt was unsuccessful), and the cooperativity length is highly impacted by the confinement effects introduced by the crystallization process [52, 24, 53]. About the other samples, the confinement effects due to crystallization are not a possible explanation for the decrease in the CRR size, since all the samples were confirmed to be in their fully amorphous state prior to measurement. The decreased CRR size could then be explained by a change in the intermolecular interactions resulting from the presence of a longer glycolic subunit in the repeating unit. Indeed, the presence of longer glycolic subunits decreases the dipole density, which in turn decreases the overall strength of the intermolecular interactions, as reported for other polymeric systems [26, 25]. The loss of inter-chain interactions due to an increased length of the glycolic subunit is more pronounced in the furan-based polyesters as compared to their terephthalic counterparts; however, this effect is only observed when the number of methylene groups increases from $n = 2$ to $n = 3$, because the presence of an additional methylene ($n = 4$) seems to have no significant effect on the value of ξ_α . In the future it would be interesting to investigate longer series of samples ($n > 4$) to confirm the possible existence of a "cooperativity threshold" at $n = 3$, beyond which the inter-chain interactions are not significantly affected by a further increase in the glycolic subunit's length.

Qin et al. [54] compiled literature data for dynamic fragility m for six types of glass-forming liquids including polymers, and showed that different categories of glass-forming liquids may exhibit different behaviours in terms of correlation between m and T_g (linear increase in m with increasing T_g for hydrogen-bonding organic, polymeric and metallic glass formers, versus a value of m almost independent of T_g for inorganic glass formers). They also pointed out a different dependence of the apparent activation energy E_g on T_g (increase to the 2^{nd} power for hydrogen-bonding organic, polymeric and metallic glass-forming liquids, versus a linear dependence for inorganic glass formers). Evans et al. [55] investigated the effect of confinement on T_g in seven polymer systems of single-layer films supported on silicon substrates (i.e. with no substantial substrate interactions) and concluded that fragility is a key variable governing the extent

of T_g -confinement effects, as it reflects the local packing efficiency in a polymer
 310 glass. The fragility index can be obtained from calorimetric experiments if the
 temperature dependence of the relaxation time is known [56]. This can be done
 by using the Tool–Narayanaswamy–Moynihan (TNM) equation:

$$\tau = \tau_0 \exp\left(\frac{x\Delta h^*}{RT}\right) \exp\left(\frac{(1-x)\Delta h^*}{RT_f}\right) \quad (5)$$

Where τ_0 is a pre-exponential factor, x is a non-linearity parameter, Δh^* is
 the apparent activation energy, R is the gas constant and T_f is the fictive tem-
 315 perature. In equation 5, T_f depends on the cooling rate and characterizes the
 instantaneous structure of the glass, i.e. the greater the cooling rate, the higher
 the fictive temperature [56]. The fragility index m is usually determined from
 calorimetric experiments by using equation 6:

$$m = \frac{d\ln(|\beta_c|)}{T_g \ln 10 d(1/T'_f)} \quad (6)$$

where β_c is the cooling rate and T'_f is the limiting fictive temperature. The
 320 variation of $\ln(|\beta_c|)$ as a function of $1/T'_f$ is supposed to be linear, and the slope
 of the corresponding curve is proportional to the fragility index [56].

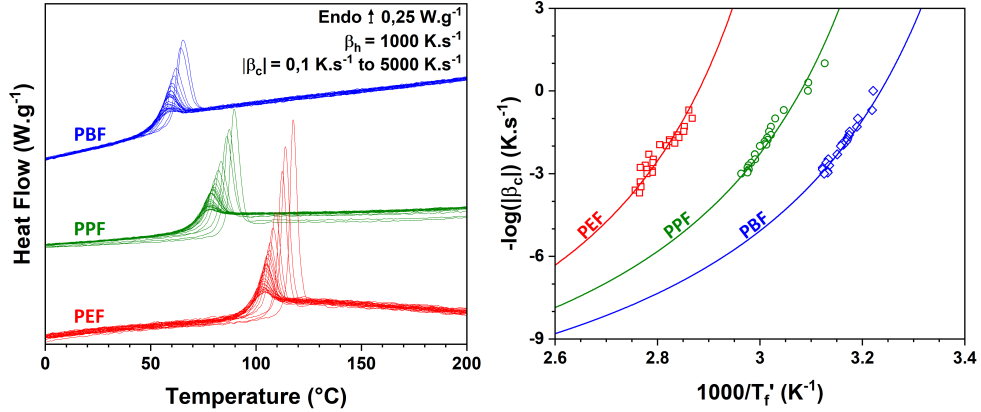


Figure 2: (Left) Heat Flow measured by FSC in the glass transition region on amorphous
 samples obtained with cooling rate ranging from 0.1 K s^{-1} to 5000 K s^{-1} for PEF, PPF,
 PBF and characterized with a heating rate $\beta_h=1000 \text{ K s}^{-1}$. (Right) Arrhenius plot of -
 $\log(|\beta_c|)$ vs. $1000/T'_f$.

Figure 2 (left) shows the Heat Flow signals recorded by FSC at a heating rate of $\beta_h = 1000Ks^{-1}$ on PEF, PPF and PBF samples cooled down from the molten state at different cooling rates ranging from $|\beta_c| = 0.1Ks^{-1}$ to $|\beta_c| = 5000Ks^{-1}$.
 325 The fictive temperature T_f has been estimated for each cooling rate β_c and the variation of $\ln(|\beta_c|)$ as a function of $1/T_f'$ has been plotted to estimate the fragility index according to equation 6. As reported in previous studies [57] and clearly shown in Figure 2, the temperature dependence of $\ln(|\beta_c|)$ follows a non-linear trend as also observed by DRS measurements (Figure 3). The temperature
 330 evolution can then be described by a Vogel-Fulcher-Tammann (VFT) equation 7:

$$\tau_\alpha(T) = \tau_\infty \exp\left(\frac{DT_0}{T - T_0}\right) \quad (7)$$

Where τ_0 is a pre-exponential factor, D is a dimensionless parameter related to the slope change (steepness strength), and T_0 is a reference temperature. A modified form of equation 7 is often used to investigate the limiting fictive
 335 temperature:

$$\ln(|\beta_c|) = A_\beta - \left(\frac{DT_0}{T_f' - T_0}\right) \quad (8)$$

Where A_β is a constant. Equation 8 was used to fit the data reported in Figure 2 and successfully followed the temperature dependence of $\ln(|\beta_c|)$. In the literature, a direct correlation between the cooling rate and the relaxation time was established using the Frenkel-Kobeko-Reiner (FKR) relationship 9 [57]:

$$|\beta_c|\tau = |\beta_c|\omega = C \quad (9)$$

340 Where $|\beta_c|$ is the cooling rate, τ is the relaxation time, and C is a constant. The FKR relationship allows to directly correlate the results obtained by FSC and the results obtained by DRS. Thus, the same VFT parameters (D and T_0) were used to fit the results obtained by FSC and DRS, with a simple logarithmic shift equal to $\log(C)$. The relaxation maps ($\log_{10} [\tau_{max}]$ as a function of
 345 $1000/T$) obtained by DRS on the fully amorphous furan-based samples are reported in Figure 3 (open symbols). Similar values of VFT fitting parameters were obtained with FSC and DRS results (Table 3). The results obtained by

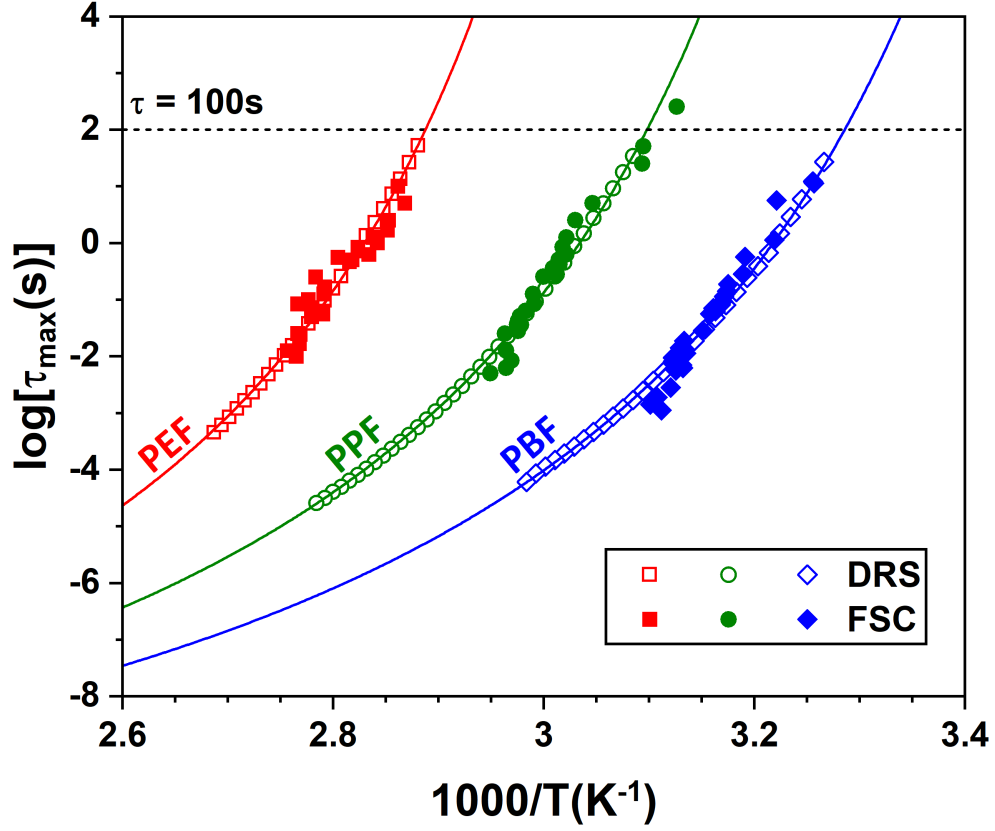


Figure 3: Relaxation maps ($\log_{10} [\tau_{max}]$) as a function of $1000/T$ obtained by both DRS and FSC on fully amorphous PEF, PPF and PBF.

FSC were shifted along the Y-axis using the $\log(C)$ values issued from the FKR equation 9, as shown in Figure 3 (close symbols). The FSC and DRS data are consistent with each other, in agreement with the results previously reported in the literature for other polymeric systems [57].

The calculation of the calorimetric fragility should be done taking into account this logarithmic shift of the temperature as a function of the cooling rate whenever the results are to be compared with DRS measurements. Therefore, equation 6 was rewritten as:

$$m = \left[\frac{d(\log\tau)}{d\left(\frac{T_g}{T}\right)} \right]_{T=T_g} \quad (10)$$

With T_g the glass transition temperature measured on a glass formed at a cooling rate $|\beta_c| = 10^{-2}$ times C . On the other hand, the dielectric fragility was calculated at a temperature T_g equal to the dielectric glass transition temperature, i.e. the temperature at which a relaxation time of $\tau = 100s$ is observed. As expected, the calorimetric and dielectric fragilities (Table 3) are in close agreement, which confirms the reliability of the two approaches and the accuracy of both the sets of experimental results.

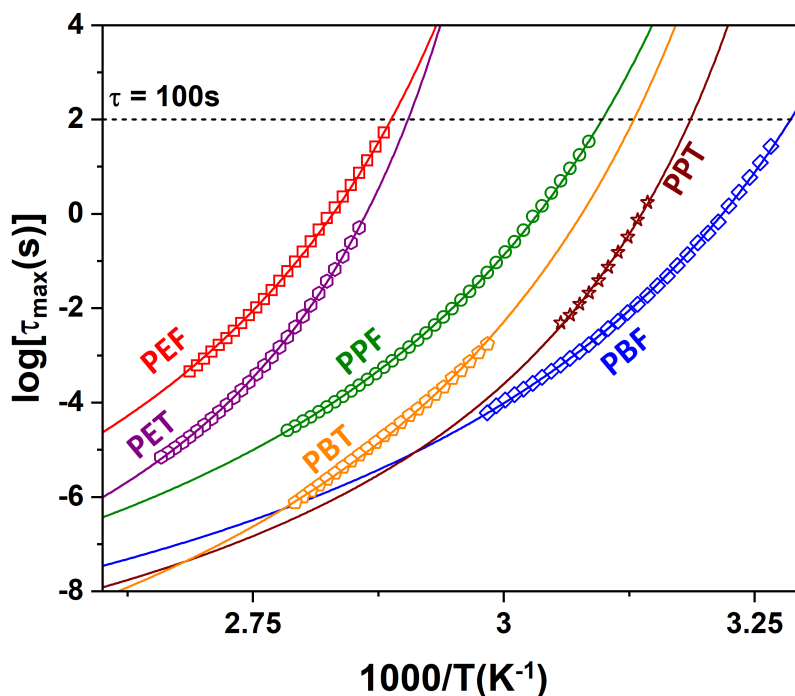


Figure 4: Relaxation maps obtained for amorphous samples of PEF, PPF, PBF, PET, PBT and PPT. The solid lines represent the best fit using VFT equation for the α -relaxation. The fitting curves of the α -relaxation have been extrapolated in order to estimate the temperature at which a relaxation time $\tau = 100s$ is observed.

The relaxation maps ($\log_{10} [\tau_{\max}]$) as a function of $1000/T$ obtained by DRS measurements performed on the fully amorphous samples (except PBT) are reported in Figure 4. All the samples show a non-linear dependence of the α -relaxation time with temperature. The VFT law (equation 7) was used to

fit the experimental data in the α -relaxation temperature range. The fragility index was estimated using Angell's equation (equation 10). The values of both $T_g(\tau = 100s)$ and the fragility index m are reported in Table 3. The fragility index is not significantly impacted by the increased length of the glycolic subunit (in agreement with the results previously reported by Soccio et al. [14]), only the value of $T_g(\tau = 100s)$ decreases. Besides, the values of the dielectric glass transition temperature are similar to the values of the calorimetric glass transition temperature determined by MT-DSC (Table 2), whose decrease has been attributed to the increased flexibility of the polymer chains. As pointed out in recent studies, the fragility index m is supposed to depend on the packing efficiency of the polymer chains in the amorphous phase [58, 59, 60] as well as on the stiffness of their backbone [30, 61, 31, 62].

If the backbone flexibility actually increases as a consequence of a longer glycolic subunit [63, 64], a decrease in the fragility index should be observed in both the furan-based and the terephthalic polyesters. However, the fragility index of the furan-based samples is constant, independently of the glycolic subunit's length. The same trend has been observed by Papamokos et al. [46] for a larger series of furan-based samples. This observation is consistent with the conclusions previously drawn by Soccio et al. [65] about PBF, asserting that fragility is mainly correlated to the molecular motions of the acidic moiety, in this case the furan ring. The literature reports that, in polymers allowing π -stacking, an increase in the glycolic subunit's length can potentially lead to a poorer packing efficiency [66]. It is therefore possible that the increased chain flexibility is compensated by a decreased packing efficiency, and that the overall fragility index remains constant for all the furan-based samples. On the other hand, in the terephthalic polyesters, a slight decrease in the fragility index is observed as the glycolic subunit's length increases, likely explained by an overall increase in chain flexibility accompanied by a slight decrease in the packing efficiency. Table 3 lists the values of fragility index obtained for both the furan-based and the terephthalic polyesters. The furan-based polymers tend to have lower values of m as compared to their terephthalic counterparts, which should mean that they are more

flexible and/or have a better chain packing efficiency according to the literature [30, 61]. However, it has been previously reported that the terephthalic samples
 400 have a more flexible backbone as compared to their furan-based counterparts [3], and that furan-based polyesters have a better chain packing efficiency as compared to their terephthalic counterparts. This difference in packing efficiency could be due to the fact that the furan ring allows π -stacking in a more efficient way than the terephthalic ring, probably because of the strong dipolar moment
 405 born by the furanic heterocycle [11].

The Kohlrausch–Williams–Watts (KWW) stretching exponent β_{KWW} is an interesting parameter that informs on the distribution of the relaxation times. According to the literature [67], it is possible to calculate the β_{KWW} stretching exponent using the following equation:

$$\beta_{KWW} = (\alpha_{HN}\beta_{HN})^{0.813} \quad (11)$$

410 Where α_{HN} and β_{HN} are the Havriliak-Negami fitting parameters. Figure 5 shows the dielectric master curves obtained for all the samples investigated in this study. No differences were observed, suggesting that the flexibility of the polymer backbone of furan-based polyesters has no significant effect on the distribution of the relaxation times. This result, combined with the invariability of
 415 the fragility index (Table 3), is supported by the expected correlation between m and the β_{KWW} stretching exponent [68, 69].

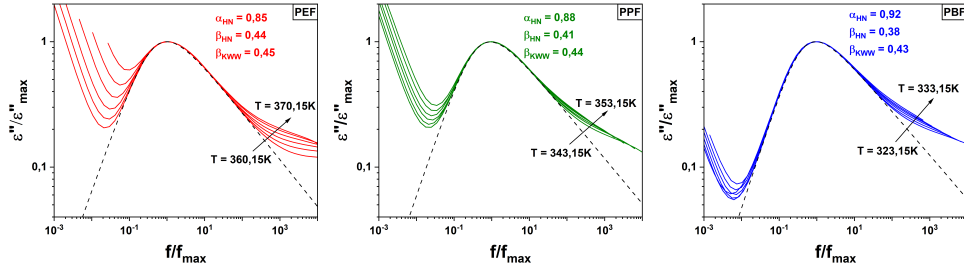


Figure 5: Dielectric master curves obtained for amorphous samples of PEF, PPF and PBF, along with the α_{HN} and β_{HN} fitting parameters. The β_{KWW} parameter has been estimated according to equation 11.

Figure 6 reports the values of fragility index versus the values of cooperativity for all the investigated samples, as well as for other samples issued from the literature [25, 26]. The theoretical domain corresponding to the volume contribution to fragility (grey area) was determined according to Hong’s equation [30] and superimposed on the experimental and literature data. For a given value of α_T/κ , if the change in fragility is only induced by a change in cooperativity, then the evolution of m correlated to the cooperativity length ξ_α should follow a linear trend. This statement is verified here in the case of the terephthalic polyesters. Their behaviour is close to the one observed in PLA with different contents of plasticizer by Araujo et al. [25]. The fact that fragility and cooperativity are correlated means that the isochoric fragility m_v is constant independently of the length of the glycolic subunit.

This behaviour is not observed in the case of the furan-based polyesters (PEF, PPF and PBF), for which fragility remains constant in spite of a change in cooperativity. A similar trend has also been reported in the case of ethylene-vinyl acetate (EVA) copolymers by Puente et al. [26]. By investigating the segmental mobility of amorphous EVA copolymers with different vinyl acetate (VAc) contents, they showed that the cooperativity decreases as the VAc content decreases (which was attributed to a decrease in the intermolecular interactions), and that the fragility remains constant whatever the VAc content. In other words, they evidenced no direct correlation between fragility and cooperativity. Figure 7 reports the isobaric and isochoric contributions to the fragility index obtained with Hong’s equation, and gives a better illustration of the variation of $m - m_v$ and m_v in both the furan-based and terephthalic polyester samples. As previously observed, the isochoric fragility m_v of the terephthalic samples does not depend on the length of the glycolic subunit (except for PBT, whose increased isochoric fragility can be explained by the presence of crystals). On the other hand, the volume contribution of the furan-based samples significantly decreases as the length of the glycolic subunit increases, which can be explained by a decrease in cooperativity. The decrease in volume contribution is accompanied by a significant increase in isochoric fragility; however, this trend is only

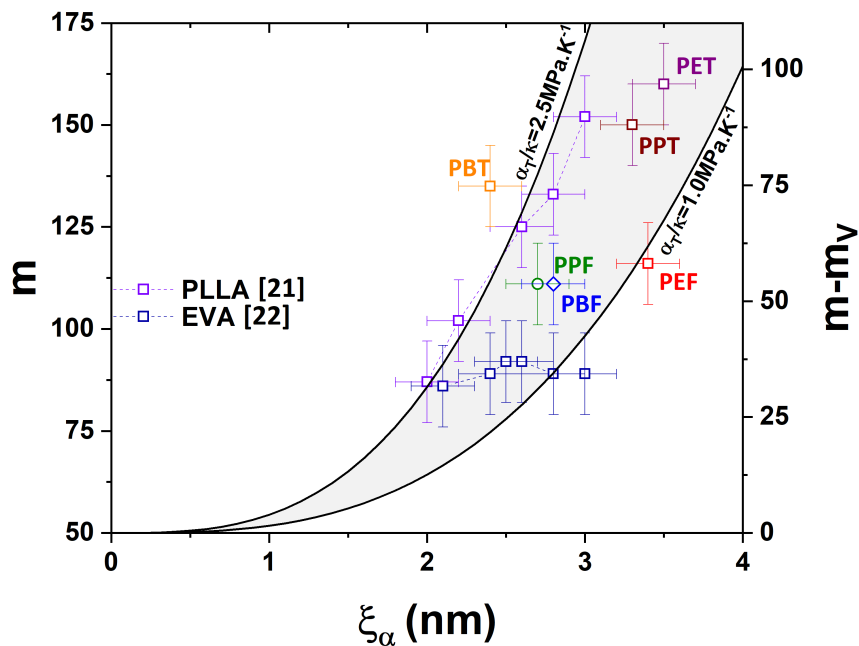


Figure 6: Fragility index versus cooperativity length for PEF, PPF and PBF as compared to PET, PTT and PBT. The data for poly(L-lactic acid) (PLLA) and ethylene-vinyl acetate (EVA) copolymers were extracted from the literature [25, 26] and added for comparison. Dashed lines are also added as a guide for the eye. The black solid lines correspond to the theoretical $m - m_v$ curves obtained with α_T/κ equal to 1.0 and 2.5 $MPa K^{-1}$ respectively, which are the extremes of the admitted range for the α_T/κ ratio according to Hong et al. [30]. The grey area represents the theoretical domain where there is a volume contribution to fragility $m - m_v$.

observed when the number of methylene groups is increased from $n = 2$ to $n = 3$, whereafter changes in the number of methylene groups has no significant effect, neither on the volume nor on the isochoric contribution. Figure 7 clearly shows that PEF and PET have similar volume contributions to the fragility index, which is expected to correlate with similar cooperativity length. However, PET shows a significantly higher isochoric fragility with respect to PEF.

According to Hong et al. [30], the isochoric fragility depends on the chemical structure of the polymer, and therefore on the type of intermolecular interactions (hydrogen-bonding, ionic or Van der Waals interactions) as well as on the

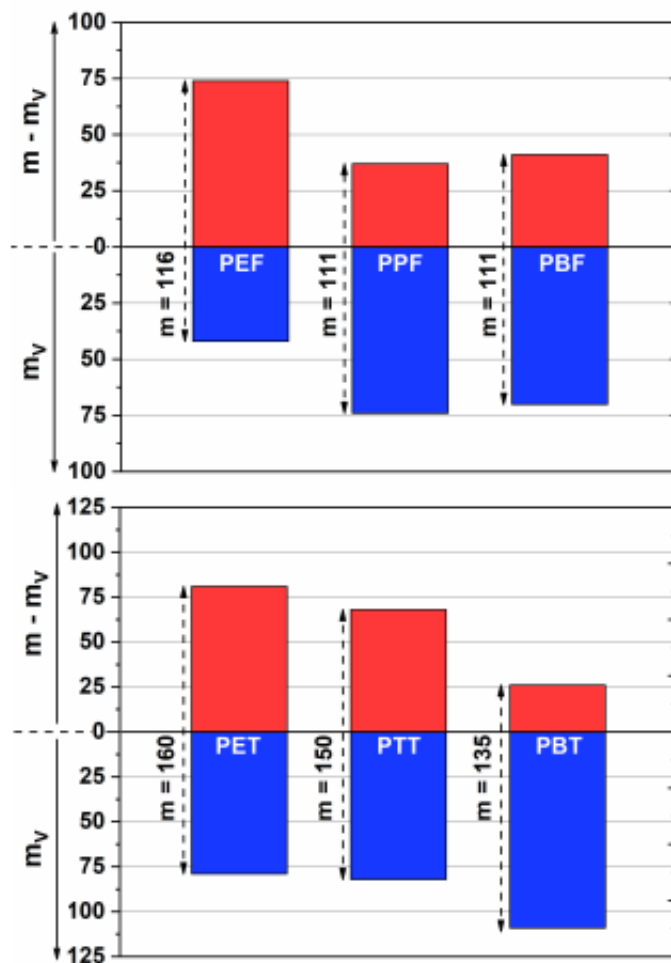


Figure 7: Colored bars represents the two fragility contributions, i.e. the volume contribution $m - m_v$ (blue) and the isochoric contribution m_v (red), calculated from experimental measurements on fully amorphous furan-based and terephthalic polyester samples. PBT is an exception, because quenching from the molten state did not yield a fully amorphous sample.

intramolecular degrees of freedom (rotational energy barriers). They showed that an increase in chain flexibility leads to a decrease in the m_v value. As previously mentioned, the two main parameters affecting the fragility index are the stiffness of the polymer backbone and the packing efficiency of the macromolecular chains [30, 61, 31].

460

to the fragility index, however PET is known to have a greater chain flexibility compared to PEF; this means that the differences observed in the m_v values might actually be attributed to strong differences in the chain packing efficiency.

465 The fact that PEF macromolecular chains have a good packing efficiency in the amorphous phase thanks to the π -stacking of the aromatic furan rings has already been reported in the literature [11, 46]. This work additionally shows that an increase in packing efficiency also leads to a significant decrease in the isochoric fragility value. This assumption is further supported by the differences

470 in isochoric fragility observed within the series of furan-based polyesters (PEF, PPF and PBF), PEF being the furan-based polyester with the highest packing efficiency. From Figure 7 it is also possible to notice that PPF and PTT have different volume contributions accompanied by different cooperativities, which is not observed when PEF is compared to PET. However, their isochoric fragili-

475 ties are similar, which can be attributed to a different backbone stiffness and chain packing efficiency, differently compensated in PPF as compared to PTT. Finally, PBT shows a very high value of isochoric fragility as compared to all the other samples; this difference could eventually be due to a much poor chain packing efficiency, but indeed no definite conclusions can be drawn because the

480 applied quenching protocol failed to achieve a fully amorphous PBT sample.

3.1. CRR (*extended Donth + extended Hong*)

The method proposed by Saiter et al.[20] combines calorimetric and dielectric experimental techniques to extend Donth's approach over a wider range of temperatures and frequencies, allowing to investigate the temperature depen-

485 dence of the CRR size. This approach was applied to the dielectric experiments performed on all the samples (except for PBT, which was not quenched to the fully amorphous state).

Figure 8 reports the evolution of the cooperativity length ξ_α as a function of the temperature normalized to the glass transition temperature obtained from

490 MT-DSC for all the samples in their fully amorphous state. A non-linear temperature dependence of the CRR size is observed in all cases, which is due to

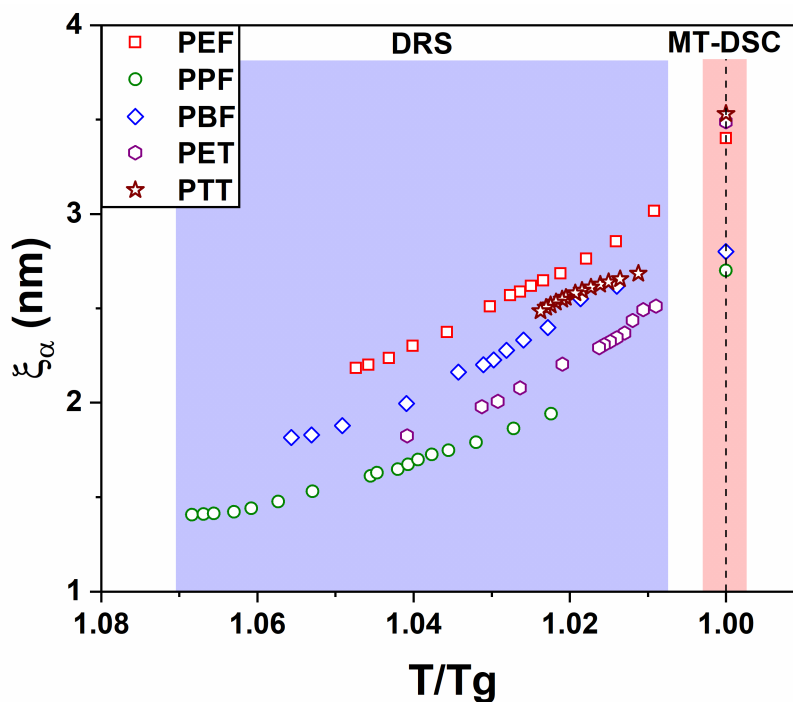


Figure 8: Values of cooperativity length (ξ_α) obtained from MT-DSC and DRS experiments for all the samples investigated in this work (PEF, PPF, PBF, PET and PTT, except for PBT that could not be quenched to the fully amorphous state) as a function of the temperature normalized to the glass transition temperature obtained from MT-DSC.

the temperature dependence of the relaxation time, as reported in the literature [70]. By combining this approach to the one proposed by Hong et al.[30], the temperature dependence of the dielectric fragility, as well as the temperature
495 dependence of the isobaric and isochoric fragilities, were estimated over a wide range of temperatures.

Figure 9 shows that the isobaric and isochoric fragilities have different temperature dependencies. A strong temperature dependence is observed for the isobaric
500 fragility, which means that its variation is thermo-activated, likely because it is directly proportional to the variation of free volume (expansion/contraction). According to previous works reported in the literature, the variations of iso-

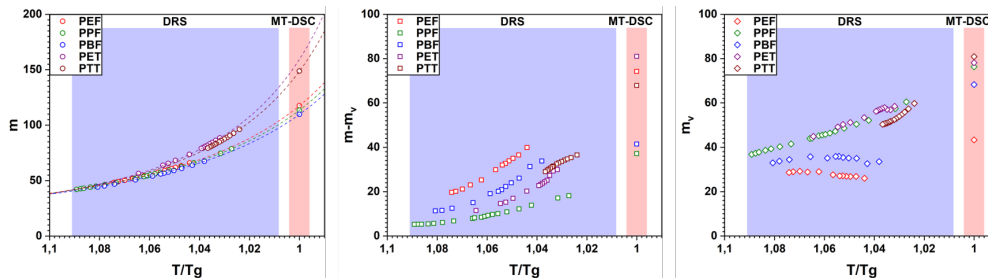


Figure 9: Dielectric (left), isobaric (middle) and isochoric (right) fragilities as a function of temperature, as estimated from the approaches proposed by Saiter et al.[20] and Hong et al.[30]. The dotted line on the left figure represents the best VFT fit.

baric fragility can be mostly attributed to changes in the inter-chain interactions [30, 61]. On the other hand, the isochoric fragility appears to be less temperature dependent, likely because its variation is mainly driven by changes in the intra-molecular interactions, that have been proved to be less affected by temperature fluctuations.

4. Conclusion

When the length of the glycolic subunit (that is to say, the number of methylene groups) in a polyester backbone increases, the inter-chain interactions decrease, thus producing a decrease in the cooperativity. This result was obtained for both furan-based and terephthalic polyesters quenched from the melt to their fully amorphous state. However, for the furan-based polyesters, no direct correlation between the fragility index and the cooperativity was observed as a consequence of the different length of their glycolic subunit. The differences in the isochoric fragilities obtained for the furan-based polyesters as compared to their terephthalic counterparts have been considered to result from a combination of backbone flexibility and packing efficiency of the macromolecular chains in the amorphous phase. An increase in chain flexibility generally leads to a decrease in isochoric fragility. However, in the case of furan-based polyesters, this can also be accompanied by a decreased packing efficiency. The comparison

of furan-based and terephthalic polyesters with different lengths of the glycolic subunit suggested that the values of isochoric fragility in the fully amorphous samples depend on both the backbone stiffness and the packing efficiency of the
525 macromolecular chains.

5. Acknowledgments

M.Soccio and N.Lotti gratefully acknowledge the support from COST Action FUR4Sustain, CA18220.

References

- 530 [1] S. Thiyagarajan, M. A. Meijlink, A. Bourdet, W. Vogelzang, R. J. I. Knoop, A. Esposito, E. Dargent, D. S. van S, J. van Haveren, Synthesis and thermal properties of bio-based copolyesters from the mixtures of 2,5- and 2,4-furandicarboxylic acid with different diols, *ACS Sustainable Chemistry Engineering* 7 (2019) 18505–18516.
535 doi:doi.org/10.1021/acssuschemeng.9b04463.
URL <https://pubs.acs.org/doi/pdf/10.1021/acssuschemeng.9b04463>
- [2] S. Thiyagarajan, A. Pukin, J. van Haveren, M. Lutz, D. S. van S, Concurrent formation of furan-2,5- and furan-2,4-dicarboxylic acid: unexpected
540 aspects of the henkel reaction, *RSC Advances* 3 (2013) 15678–15686.
doi:doi.org/10.1039/C3RA42457J.
URL <https://pubs.rsc.org/en/content/articlehtml/2013/ra/c3ra42457j>
- [3] S. K. Burgess, J. E. Leisen, B. E. Kraftschik, C. R. Mubarak, R. M.
545 Kriegel, W. J. Koros, Chain mobility, thermal, and mechanical properties of poly(ethylene furanoate) compared to poly(ethylene terephthalate), *Macromolecules* 47 (4) (2014) 1383–1391. doi:10.1021/ma5000199.
URL <https://pubs.acs.org/doi/10.1021/ma5000199>

- [4] F. Nederberg, R. L. Bell, J. M. Torradas, Furan-based polymeric hydrocarbon fuel barrier structures.
550 URL <https://patents.google.com/patent/US20160311208A1/en>
- [5] M. Soccio, M. Costa, N. Lotti, M. Gazzano, V. Siracusa, E. Salatelli, P. Manaresi, A. Munari, Novel fully biobased poly(butylene 2,5-furanoate/diglycolate) copolymers containing ether linkages: Structure-property relationships, *European Polymer Journal* 81 (2016) 397–412.
555 doi:doi.org/10.1016/j.eurpolymj.2016.06.022.
URL <https://www.sciencedirect.com/science/article/pii/S0014305716304499>
- [6] I. Kolesov, R. Androsch, The rigid amorphous fraction of cold-crystallized polyamide 6, *Polymer* 53 (21) (2012) 4770–4777.
560 doi:10.1016/j.polymer.2012.08.017.
URL <https://linkinghub.elsevier.com/retrieve/pii/S0032386112006799>
- [7] M. L. Di Lorenzo, M. C. Righetti, The three-phase structure of isotactic poly(1-butene), *Polymer* 49 (5) (2008) 1323–1331.
565 doi:10.1016/j.polymer.2008.01.026.
URL <https://linkinghub.elsevier.com/retrieve/pii/S0032386108000827>
- [8] B. G. Olson, J. Lin, S. Nazarenko, A. M. Jamieson, Positron annihilation lifetime spectroscopy of poly(ethylene terephthalate): Contributions from rigid and mobile amorphous fractions, *Macromolecules* 36 (20) (2003) 7618–7623. doi:10.1021/ma034813u.
570 URL <http://pubs.acs.org/doi/abs/10.1021/ma034813u>
- [9] A. Guinault, C. Sollogoub, V. Ducruet, S. Domenek, Impact of crystallinity of poly(lactide) on helium and oxygen barrier properties, *European Polymer Journal* 48 (4) (2012) 779–788.
575 doi:10.1016/j.eurpolymj.2012.01.014.

URL <http://linkinghub.elsevier.com/retrieve/pii/S0014305712000304>

- 580 [10] A. Esposito, N. Delpouve, V. Causin, A. Dhotel, L. Delbreilh, E. Dargent, From a three-phase model to a continuous description of molecular mobility in semicrystalline poly(hydroxybutyrate-co-hydroxyvalerate), *Macromolecules* 49 (13) (2016) 4850–4861. doi:10.1021/acs.macromol.6b00384.

585 URL <http://pubs.acs.org/doi/10.1021/acs.macromol.6b00384>

- [11] A. Bourdet, A. Esposito, S. Thiyagarajan, L. Delbreilh, F. Affouard, R. J. I. Knoop, E. Dargent, Molecular mobility in amorphous biobased poly(ethylene 2,5-furandicarboxylate) and poly(ethylene 2,4-furandicarboxylate), *Macromolecules* 51 (5) (2018) 1937–1945. doi:10.1021/acs.macromol.8b00108.

590 URL <http://pubs.acs.org/doi/10.1021/acs.macromol.8b00108>

- [12] A. Bourdet, S. Araujo, S. Thiyagarajan, L. Delbreilh, A. Esposito, E. Dargent, Molecular mobility in amorphous biobased copolyesters obtained with 2,5- and 2,4-furandicarboxylate acid, *Polymer* 213 (2021) 123225. doi:10.1016/j.polymer.2020.123225.

595 URL <https://www.sciencedirect.com/science/article/pii/S0032386120310508>

- [13] G. Guidotti, M. Soccio, M. García-Gutiérrez, V. Ezquerra, T. Siracusa, E. Gutiérrez-Fernández, A. Munari, N. Lotti, Fully biobased superpolymers of 2,5-furandicarboxylic acid with different functional properties: From rigid to flexible, high performant packaging materials, *ACS Sustainable Chemistry & Engineering* 8 (25) (2020) 9558–9568. doi:10.1021/acssuschemeng.0c02840.

600 URL <https://doi.org/10.1021/acssuschemeng.0c02840>

- 605 [14] M. Soccio, D. E. Martínez-Tong, G. Guidotti, B. Robles-Hernández, A. Munari, N. Lotti, A. Alegria, Broadband dielectric spectroscopy study

of biobased poly(alkylene 2,5-furanoate)s' molecular dynamics, *Polymers* 12 (6) (2020) 1355. doi:10.3390/polym12061355.

URL <https://www.mdpi.com/2073-4360/12/6/1355>

- 610 [15] D. E. Martínez-Tong, M. Soccio, B. Robles-Hernández, G. Guidotti, M. Gazzano, N. Lotti, A. Alegria, Evidence of nanostructure development from the molecular dynamics of poly(pentamethylene 2,5-furanoate), *Macromolecules* 53 (23) (2020) 10526–10537. doi:10.1021/acs.macromol.0c02297.

615 URL <https://doi.org/10.1021/acs.macromol.0c02297>

- [16] L. Genovese, M. Soccio, N. Lotti, A. Munari, A. Szymczyk, S. Paszkiewicz, A. Linares, A. Nogales, T. Ezquerra, Effect of chemical structure on the subglass relaxation dynamics of biobased polyesters as revealed by dielectric spectroscopy: 2,5-furandicarboxylic acid vs. trans-1,4-cyclohexanedicarboxylic acid, *Physical Chemistry Chemical Physics* 20 (2018) 15696–15706. doi:10.1039/C8CP01810C.

620 URL <https://pubs.rsc.org/en/content/articlelanding/2018/cp/c8cp01810c>

- [17] G. Adam, J. H. Gibbs, On the temperature dependence of cooperative relaxation properties in glass-forming liquids, *The Journal of Chemical Physics* 43 (1) (1965) 139–146. doi:10.1063/1.1696442.

625 URL <http://aip.scitation.org/doi/10.1063/1.1696442>

- [18] E. Donth, The size of cooperatively rearranging regions at the glass transition, *Journal of Non-Crystalline Solids* 53 (3) (1982) 325–330. doi:10.1016/0022-3093(82)90089-8.

630 URL <https://linkinghub.elsevier.com/retrieve/pii/S0022309382900898>

- [19] E. Donth, Characteristic length of the glass transition, *Journal of Polymer Science Part B: Polymer Physics* 34 (17) (1996) 2881–2892. doi:10.1002/(SICI)1099-0488(199612)34:17<2881::

635

AID-POLB3>3.0.CO;2-U.

URL [https://doi.org/10.1002/\(SICI\)1099-0488\(199612\)34:17<2881::AID-POLB3>3.0.CO;2-U](https://doi.org/10.1002/(SICI)1099-0488(199612)34:17<2881::AID-POLB3>3.0.CO;2-U)

- [20] A. Saiter, L. Delbreilh, H. Couderc, K. Arabeche, A. Schönhals, J.-M. Saiter, Temperature dependence of the characteristic length scale for glassy dynamics: Combination of dielectric and specific heat spectroscopy, *Physical Review E* 81 (4) (2010) 041805. doi:10.1103/PhysRevE.81.041805. URL <https://link.aps.org/doi/10.1103/PhysRevE.81.041805>
- [21] A. Saiter, D. Prevosto, E. Passaglia, H. Couderc, L. Delbreilh, J. M. Saiter, Cooperativity length scale in nanocomposites: Interfacial and confinement effects, *Physical Review E* 88 (4) (2013) 042605. doi:10.1103/PhysRevE.88.042605. URL <https://link.aps.org/doi/10.1103/PhysRevE.88.042605>
- [22] C. Zhang, Y. Guo, R. D. Priestley, Characteristic length of the glass transition in isochorically confined polymer glasses, *ACS Macro Letters* 3 (6) (2014) 501–505. doi:10.1021/mz500204q. URL <https://pubs.acs.org/doi/10.1021/mz500204q>
- [23] K. Arabeche, L. Delbreilh, J.-M. Saiter, G. Michler, R. Adhikari, E. Baer, Fragility and molecular mobility in micro- and nano-layered pc/pmma films, *Polymer* 55 (6) (2014) 1546–1551. doi:10.1016/j.polymer.2014.02.006. URL <https://linkinghub.elsevier.com/retrieve/pii/S0032386114000925>
- [24] X. Monnier, L. Chevalier, A. Esposito, L. Fernandez-Ballester, A. Saiter, E. Dargent, Local and segmental motions of the mobile amorphous fraction in semi-crystalline polylactide crystallized under quiescent and flow-induced conditions, *Polymer* 126 (2017) 141–151. doi:10.1016/j.polymer.2017.08.021.

- URL <https://www.sciencedirect.com/science/article/pii/S0032386117307942>
665
- [25] S. Araujo, N. Delpouve, S. Domenek, A. Guinault, R. Golovchak, R. Szatanik, A. Ingram, C. Fauchard, L. Delbreilh, E. Dargent, Cooperativity scaling and free volume in plasticized polylactide, *Macromolecules* 52 (16) (2019) 6107–6115. doi:10.1021/acs.macromol.9b00464.
670 URL <https://pubs.acs.org/doi/10.1021/acs.macromol.9b00464>
- [26] J. Puente, B. Rijal, L. Delbreilh, K. Fatyeyeva, A. Saiter, E. Dargent, Segmental mobility and glass transition of poly(ethylene-vinyl acetate) copolymers: Is there a continuum in the dynamic glass transitions from pvac to pe?, *Polymer* 76 (2015) 213–219. doi:10.1016/j.polymer.2015.09.007.
675 URL <https://linkinghub.elsevier.com/retrieve/pii/S0032386115302123>
- [27] X. Monnier, N. Delpouve, N. Basson, A. Guinault, S. Domenek, A. Saiter, P. Mallon, E. Dargent, Molecular dynamics in electrospun amorphous plasticized polylactide fibers, *Polymer* 73 (2015) 68–78.
680 doi:10.1016/j.polymer.2015.07.047.
URL <https://linkinghub.elsevier.com/retrieve/pii/S0032386115301294>
- [28] E. Bouthegourd, A. Esposito, D. Lourdin, S. A., S. J.M., Size of the cooperative rearranging regions versus fragility in complex glassy systems: influence of the structure and the molecular interactions, *Physica B: Condensed Matter* 425 (2013) 83–89. doi:10.1016/j.physb.2013.05.029.
685 URL <https://www.sciencedirect.com/science/article/pii/S0921452613003426>
- [29] M. Nakanishi, R. Nozaki, Model of the cooperative rearranging region for polyhydric alcohols, *Physical Review E* 84 (1) (2011) 011503. doi:10.1103/PhysRevE.84.011503.
690 URL <https://link.aps.org/doi/10.1103/PhysRevE.84.011503>

- [30] L. Hong, V. Novikov, A. Sokolov, Is there a connection between fragility of glass forming systems and dynamic heterogeneity/cooperativity?, *Journal of Non-Crystalline Solids* 357 (2) (2011) 351–356. doi:10.1016/j.jnoncrysol.2010.06.071.
695
URL <https://linkinghub.elsevier.com/retrieve/pii/S0022309310005259>
- [31] S. Araujo, F. Batteux, W. Li, L. Butterfield, N. Delpouve, A. Esposito, L. Tan, J.-M. Saiter, M. Negahban, A structural interpretation of the two components governing the kinetic fragility from the example of interpenetrated polymer networks: A structural interpretation of the two components governing the kinetic fragility from the example of interpenetrated polymer networks, *Journal of Polymer Science Part B: Polymer Physics* 56 (20) (2018) 1393–1403. doi:10.1002/polb.24722.
700
URL <http://doi.wiley.com/10.1002/polb.24722>
- [32] S. Thiyagarajan, W. Vogelzang, R. J. I. Knoop, A. E. Frissen, J. v. Haveren, D. S. v. Es, Biobased furandicarboxylic acids (fdcas): effects of isomeric substitution on polyester synthesis and properties, *Green Chemistry* 16 (4) (2014) 1957–1966, publisher: The Royal Society of Chemistry. doi:10.1039/C3GC42184H.
710
URL <https://pubs.rsc.org/en/content/articlelanding/2014/gc/c3gc42184h>
- [33] C. Fosse, A. Bourdet, E. Ernault, A. Esposito, N. Delpouve, L. Delbreilh, S. Thiyagarajan, R. J. Knoop, E. Dargent, Determination of the equilibrium enthalpy of melting of two-phase semi-crystalline polymers by fast scanning calorimetry, *Thermochimica Acta* 677 (2019) 67–78. doi:10.1016/j.tca.2019.03.035.
715
URL <https://linkinghub.elsevier.com/retrieve/pii/S004060311831102X>
720
- [34] R. J. I. Knoop, W. Vogelzang, J. van Haveren, D. S. van Es, High molec-

ular weight poly(ethylene-2,5-furanoate); critical aspects in synthesis and mechanical property determination, *Journal of Polymer Science, Part A: Polymer Chemistry* 51 (2013) 4191–4199. doi:10.1002/pola.26833.

725 URL <https://onlinelibrary.wiley.com/doi/10.1002/pola.26833>

- [35] G. Guidotti, M. Soccio, N. Lotti, M. Gazzano, V. Siracusa, A. Munari, Poly(propylene 2,5-thiophenedicarboxylate) vs. poly(propylene 2,5-furandicarboxylate): Two examples of high gas barrier bio-based polyesters, *Polymers* 10 (7) (2018) 785, number: 7 Publisher: Multidisciplinary Digital Publishing Institute. doi:10.3390/polym10070785.

730 URL <https://www.mdpi.com/2073-4360/10/7/785>

- [36] A. A. Lacey, D. M. Price, M. Reading, Theory and practice of modulated temperature differential scanning calorimetry, in: M. Reading, D. J. Hourston (Eds.), *Modulated Temperature Differential Scanning Calorimetry*, Vol. 6, Springer Netherlands, 2006, pp. 1–81. doi:10.1007/1-4020-3750-3_1.

735 URL http://link.springer.com/10.1007/1-4020-3750-3_1

- [37] J. E. Schawe, Measurement of the thermal glass transition of polystyrene in a cooling rate range of more than six decades, *Thermochimica Acta* 603 (2015) 128–134. doi:10.1016/j.tca.2014.05.025.

740 URL <https://linkinghub.elsevier.com/retrieve/pii/S0040603114002305>

- [38] A. Toda, R. Androsch, C. Schick, Insights into polymer crystallization and melting from fast scanning chip calorimetry, *Polymer* 91 (2016) 239–263. doi:10.1016/j.polymer.2016.03.038.

745 URL <http://linkinghub.elsevier.com/retrieve/pii/S0032386116301781>

- [39] K. Jariyavidyanont, A. Abdelaziz, R. Androsch, C. Schick, Experimental analysis of lateral thermal inhomogeneity of a specific chip-calorimeter sensor, *Thermochimica Acta* 674 (2019) 95–99.

750

doi:10.1016/j.tca.2019.02.016.

URL <https://linkinghub.elsevier.com/retrieve/pii/S0040603119300693>

[40] S. Havriliak, S. Negami, A complex plane analysis of alpha-dispersions in some polymer systems, Journal of Polymer Science Part C: Polymer Symposia 14 (1) (1966) 99–117. arXiv:<https://onlinelibrary.wiley.com/doi/pdf/10.1002/polc.5070140111>, doi:<https://doi.org/10.1002/polc.5070140111>.
URL <https://onlinelibrary.wiley.com/doi/abs/10.1002/polc.5070140111>

[41] S. Havriliak, S. Negami, A complex plane representation of dielectric and mechanical relaxation processes in some polymers, Polymer 8 (1967) 161–210. doi:[https://doi.org/10.1016/0032-3861\(67\)90021-3](https://doi.org/10.1016/0032-3861(67)90021-3).
URL <https://www.sciencedirect.com/science/article/pii/0032386167900213>

[42] J. Zhu, J. Cai, W. Xie, P.-H. Chen, M. Gazzano, M. Scandola, R. A. Gross, Poly(butylene 2,5-furan dicarboxylate), a biobased alternative to pbt: Synthesis, physical properties, and crystal structure, Macromolecules 46 (3) (2013) 796–804. doi:10.1021/ma3023298.
URL <http://pubs.acs.org/doi/10.1021/ma3023298>

[43] G. Z. Papageorgiou, V. Tsanaktsis, D. G. Papageorgiou, S. Exarhopoulos, M. Papageorgiou, D. N. Bikiaris, Evaluation of polyesters from renewable resources as alternatives to the current fossil-based polymers. phase transitions of poly(butylene 2,5-furan-dicarboxylate), Polymer 55 (16) (2014) 3846–3858. doi:10.1016/j.polymer.2014.06.025.
URL <http://linkinghub.elsevier.com/retrieve/pii/S0032386114005199>

[44] L. Martino, N. Guigo, J. G. van Berkel, J. J. Kolstad, N. Sbirrazzoli, Nucleation and self-nucleation of bio-based poly(ethylene 2,5-

780 furandicarboxylate) probed by fast scanning calorimetry, *Macromolecular
Materials and Engineering* 301 (5) (2016) 586–596. doi:10.1002/mame.
201500418.

URL <http://doi.wiley.com/10.1002/mame.201500418>

[45] M. C. Righetti, P. Marchese, M. Vannini, A. Celli, F. Tricoli, C. Lorenzetti,
785 Temperature-induced polymorphism in bio-based poly(propylene
2,5-furandicarboxylate), *Thermochimica Acta* 677 (2019) 186–193.
doi:10.1016/j.tca.2018.12.003.

URL [https://linkinghub.elsevier.com/retrieve/pii/
S0040603118307779](https://linkinghub.elsevier.com/retrieve/pii/S0040603118307779)

790 [46] G. Papamokos, T. Dimitriadis, D. N. Bikiaris, G. Z. Papageorgiou,
G. Floudas, Chain conformation, molecular dynamics, and thermal prop-
erties of poly(*n*-methylene 2,5-furanoates) as a function of methylene
unit sequence length, *Macromolecules* 52 (17) (2019) 6533–6546. doi:
10.1021/acs.macromol.9b01320.

795 URL <https://pubs.acs.org/doi/10.1021/acs.macromol.9b01320>

[47] J. Örtengren, J. Tidlund, M. Nykvist, P. Busson, A. Hult, S. Sen, R. Boyd,
U. Gedde, Dielectric relaxation of liquid crystalline dendrimers and liquid
crystalline polymers with pendant nitro groups, *Polymer* 42 (25) (2001)
10027–10033. doi:10.1016/S0032-3861(01)00558-4.

800 URL [https://linkinghub.elsevier.com/retrieve/pii/
S0032386101005584](https://linkinghub.elsevier.com/retrieve/pii/S0032386101005584)

[48] J. G. Smith, C. J. Kibler, B. J. Sublett, Preparation and properties
of poly(methylene terephthalates), *Journal of Polymer Science Part A-
1: Polymer Chemistry* 4 (7) (1966) 1851–1859. doi:10.1002/pol.1966.
805 150040719.

URL <http://doi.wiley.com/10.1002/pol.1966.150040719>

[49] M. Soccio, N. Lotti, L. Finelli, M. Gazzano, A. Munari, Aliphatic
poly(propylene dicarboxylate)s: Effect of chain length on thermal prop-

- erties and crystallization kinetics, *Polymer* 48 (11) (2007) 3125–3136.
810 doi:10.1016/j.polymer.2007.04.007.
URL <https://linkinghub.elsevier.com/retrieve/pii/S0032386107003564>
- [50] E. Hempel, G. Hempel, A. Hensel, C. Schick, E. Donth, Characteristic length of length glass transition near T_g for a wide assortment of glass-
815 forming substances, *The Journal of Physical Chemistry B* 104 (11) (2000) 2460–2466. doi:10.1021/jp991153f.
URL <https://pubs.acs.org/doi/10.1021/jp991153f>
- [51] E. Donth, H. Huth, M. Beiner, Characteristic length of the glass transition, *Journal of Physics: Condensed Matter* 13 (22) (2001) L451–L462.
820 doi:10.1088/0953-8984/13/22/102.
URL <http://stacks.iop.org/0953-8984/13/i=22/a=102?key=crossref.2b77ff4963be2037d57b8a1678cf867a>
- [52] N. Varol, N. Delpouve, S. Araujo, S. Domenek, A. Guinault, R. Golovchak, A. Ingram, L. Delbreilh, E. Dargent, Amorphous rigidification and cooper-
825 ativity drop in semi-crystalline plasticized polylactide, *Polymer* 194 (2020) 122373. doi:10.1016/j.polymer.2020.122373.
URL <https://linkinghub.elsevier.com/retrieve/pii/S003238612030210X>
- [53] C. Schick, E. Donth, Characteristic length of glass transition: experimental evidence, *Physica Scripta* 43 (4) (1991) 423–429.
830 doi:10.1088/0031-8949/43/4/010.
URL <http://stacks.iop.org/1402-4896/43/i=4/a=010?key=crossref.439c59105109271136978e9eab6a28f8>
- [54] Q. Qin, G. B. McKenna, Correlation between dynamic fragility and
835 glass transition temperature for different classes of glass forming liquids, *Journal of Non-Crystalline Solids* 352 (28) (2006) 2977–2985.
doi:10.1016/j.jnoncrysol.2006.04.014.

URL <https://www.sciencedirect.com/science/article/pii/S0022309306005898>

- 840 [55] C. M. Evans, H. Deng, W. F. Jager, J. M. Torkelson, Fragility is a key parameter in determining the magnitude of tg-confinement effects in polymer films, *Macromolecules* 46 (15) (2013) 6091–6103, publisher: American Chemical Society. doi:10.1021/ma401017n.

URL <https://doi.org/10.1021/ma401017n>

- 845 [56] L. Delbreilh, M. Negahban, M. Benzohra, C. Lacabanne, J. Saiter, Glass transition investigated by a combined protocol using thermostimulated depolarization currents and differential scanning calorimetry, *Journal of Thermal Analysis and Calorimetry* 96 (3) (2009) 865 – 871. doi:10.1007/s10973-009-0060-1.

850 URL <https://akjournals.com/view/journals/10973/96/3/article-p865.xml>

- [57] A. Dhotel, B. Rijal, L. Delbreilh, E. Dargent, A. Saiter, Combining flash dsc, dsc and broadband dielectric spectroscopy to determine fragility, *Journal of Thermal Analysis and Calorimetry* 121 (25) (2015) 453–461. doi:doi.org/10.1007/s10973-015-4650-9.

855 URL <https://https://link.springer.com/article/10.1007/s10973-015-4650-9#citeas>

- [58] J. Dudowicz, K. F. Freed, J. F. Douglas, Fragility of glass-forming polymer liquids, *The Journal of Physical Chemistry B* 109 (45) (2005) 21350–21356, pMID: 16853769. arXiv:<https://doi.org/10.1021/jp053693k>, doi:10.1021/jp053693k.

860 URL <https://doi.org/10.1021/jp053693k>

- [59] J. Dudowicz, K. F. Freed, J. F. Douglas, The glass transition temperature of polymer melts, *The Journal of Physical Chemistry B* 109 (45) (2005) 21285–21292, pMID: 16853759. arXiv:<https://doi.org/10.1021/jp0523266>,

865

doi:10.1021/jp0523266.

URL <https://doi.org/10.1021/jp0523266>

- [60] J. Wu, G. Huang, L. Qu, J. Zheng, Correlations between dynamic fragility and dynamic mechanical properties of several amorphous polymers, *Journal of Non-Crystalline Solids* 355 (34) (2009) 1755 – 1759. doi:<https://doi.org/10.1016/j.jnoncrysol.2009.06.013>.
URL <http://www.sciencedirect.com/science/article/pii/S0022309309003470>
- [61] K. Kunal, C. G. Robertson, S. Pawlus, S. F. Hahn, A. P. Sokolov, Role of chemical structure in fragility of polymers: A qualitative picture, *Macromolecules* 41 (19) (2008) 7232–7238. doi:10.1021/ma801155c.
URL <https://pubs.acs.org/doi/10.1021/ma801155c>
- [62] R. Kumar, M. Goswami, B. G. Sumpter, V. N. Novikov, A. P. Sokolov, Effects of backbone rigidity on the local structure and dynamics in polymer melts and glasses, *Physical Chemistry Chemical Physics* 15 (13) (2013) 4604. doi:10.1039/c3cp43737j.
URL <http://xlink.rsc.org/?DOI=c3cp43737j>
- [63] P. G. Santangelo, C. M. Roland, Molecular weight dependence of fragility in polystyrene, *Macromolecules* 31 (14) (1998) 4581–4585. arXiv:<https://doi.org/10.1021/ma971823k>, doi:10.1021/ma971823k.
URL <https://doi.org/10.1021/ma971823k>
- [64] M. L. Williams, R. F. Landel, J. D. Ferry, The temperature dependence of relaxation mechanisms in amorphous polymers and other glass-forming liquids, *J. Am. Chem. Soc.* 77 (14) (1955) 3701–3707. doi:10.1021/ja01619a008.
URL <https://pubs.acs.org/doi/abs/10.1021/ja01619a008>
- [65] M. Soccio, D. E. Martínez-Tong, A. Alegría, A. Munari, N. Lotti, Molecular dynamics of fully biobased poly(butylene 2,5-furanoate) as

- revealed by broadband dielectric spectroscopy, *Polymer* 128 (2017) 24–30.
895 doi:10.1016/j.polymer.2017.09.007.
URL [http://linkinghub.elsevier.com/retrieve/pii/
S0032386117308698](http://linkinghub.elsevier.com/retrieve/pii/S0032386117308698)
- [66] Z. Ma, H. Geng, D. Wang, Z. Shuai, Influence of alkyl side-chain length
on the carrier mobility in organic semiconductors: herringbone vs. pi–pi
900 stacking, *Journal of Materials Chemistry C* 4 (20) (2016) 4546–4555. doi:
10.1039/C6TC00755D.
URL <http://xlink.rsc.org/?DOI=C6TC00755D>
- [67] A. Schönhals, F. Kremer, Theory of dielectric relaxation, in: *Broadband
Dielectric Spectroscopy*, Springer, Berlin, Heidelberg, 2003, pp. 1–33.
905 doi:10.1007/978-3-642-56120-7_1.
URL [https://link.springer.com/chapter/10.1007/
978-3-642-56120-7_1](https://link.springer.com/chapter/10.1007/978-3-642-56120-7_1)
- [68] M. Ikeda, M. Aniya, Correlation between fragility and cooperativity in bulk
metallic glass-forming liquids, *Intermetallics* 18 (10) (2010) 1796–1799.
910 doi:10.1016/j.intermet.2010.01.009.
URL [https://www.sciencedirect.com/science/article/pii/
S0966979510000208](https://www.sciencedirect.com/science/article/pii/S0966979510000208)
- [69] T. A. Vilgis, Strong and fragile glasses: A powerful classification and
its consequences, *Physical Review B* 47 (5) (1993) 2882–2885, publisher:
915 American Physical Society. doi:10.1103/PhysRevB.47.2882.
URL <https://link.aps.org/doi/10.1103/PhysRevB.47.2882>
- [70] B. Rijal, L. Delbreilh, A. Saiter, Dynamic heterogeneity and coopera-
tive length scale at dynamic glass transition in glass forming liquids,
Macromolecules 48 (22) (2015) 8219–8231. doi:10.1021/acs.macromol.
920 5b01152.
URL <https://pubs.acs.org/doi/10.1021/acs.macromol.5b01152>

Table 1: List of the furan-based polyesters and their terephthalic counterparts, with indication of the source, the number-average molecular weight (\overline{M}_n) and the weight-average molecular weight (\overline{M}_w).

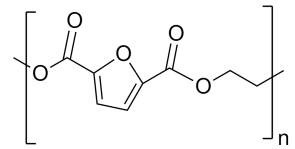
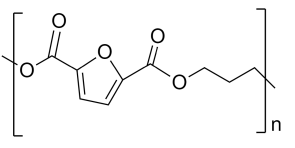
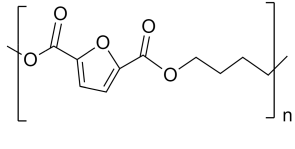
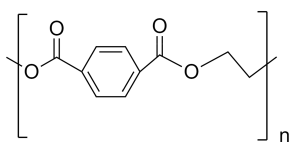
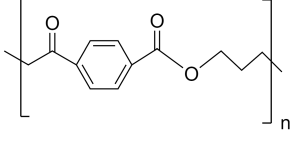
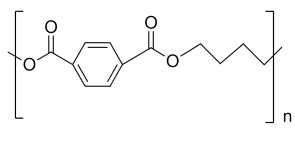
SAMPLE	REPETITIVE UNIT	SOURCE	\overline{M}_n ($gmol^{-1}$)	\overline{M}_w ($gmol^{-1}$)
PEF		FBR, Wageningen The Netherlands	15 300	18 200
PPF		DICAM, Bologna Italy	n.a	62 000
PBF		FBR, Wageningen The Netherlands	36 000	74 500
PET		Carolex Co.	31 000	62 000
PTT		FBR, Wageningen The Netherlands	16 500	30 500
PBT		Celanex 2500 Hoechst Co.	20 000 to 35 000	n.a.

Table 2: Thermal parameters extracted from the MT-DSC curves in Figure 1. T_g is the glass transition temperature measured as the midpoint of the glass transition. T_c and T_m are respectively the cold crystallization and melting temperatures measured at the maximum of the peak. δT_{cc} is the width of the cold crystallization peak measured as the difference between the onset and endset temperatures. ΔT_g and ΔC_p^0 are the width of the glass transition and the Heat Capacity step change at the glass transition temperature estimated from the Reversing Heat Capacity signal using the 16-84% method by Hempel et al. [50]. T_α and δT_g are respectively the temperature and the width of the α -relaxation peak observed on the Non-Reversing Heat Capacity signal. ξ_α is the cooperativity length at the dynamic glass transition estimated according to Donth's model[18, 51].

SAMPLE	T_g ± 1 [°C]	ΔT_g ± 1 [°C]	ΔC_p^0 ± 0.01 [$J g^{-1} \cdot ^\circ C^{-1}$]	T_α ± 1 [°C]	δT_g ± 1 [°C]	ξ_α ± 0.1 [nm]
PEF	83	6.8	0.39	82	2.8	3.4
PPF	57	7.7	0.37	56	2.6	2.7
PBF	38	4.3	0.33	38	2.6	2.8
PET	80	4.7	0.32	79	2.1	3.5
PPT	47	3.9	0.36	44	2.1	3.3
PBT	43	13.5	n.d	41	4.7	2.4

Table 3: Parameters obtained with the VFT fitting procedure applied to DRS experimental curves. T_g ($\tau=100s$) is the dielectric glass transition temperature, i.e. the temperature at which a relaxation time of 100s is observed, m is the fragility index, $(m - m_v)$ and m_v are the isobaric and the isochoric fragilities, respectively.

SAMPLE	FSC			DRS			
	$\log(C)$	$T_g(\beta_c = 10^{-2}C) \pm 1$ [°C]	m	$T_g(\tau = 100s) \pm 1$ [°C]	m	$m - m_v$	m_v
PEF	1.7	75	105	73	116	74	42
PPF	1.4	54	94	58	111	37	74
PBF	1.5	38	96	37	111	41	70
PET	n.a	n.a	n.a	71	160	81	79
PPT	n.a	n.a	n.a	40	150	68	82
PBT	n.a	n.a	n.a	46	135	26	109